

Fabrication of subwavelength periodic nanostructures using liquid immersion Lloyd's mirror interference lithography

Abhijeet Bagal and Chih-Hao Chang*

Department of Mechanical and Aerospace Engineering, North Carolina State University, Raleigh, North Carolina 27695, USA

*Corresponding author: chichang@ncsu.edu

Received May 17, 2013; accepted June 10, 2013;

posted June 18, 2013 (Doc. ID 190685); published July 10, 2013

We have developed a liquid immersion Lloyd's mirror interference lithography system to fabricate subwavelength periodic nanostructures. In this approach, we construct the Lloyd's mirror interferometer within a liquid medium to increase the ambient index. The light wavelength is scaled by the refractive index of the immersion fluid, reducing the minimum interference pattern period and increasing the spatial resolution. The all-liquid system ensures continuous fluid contact with the sample without an external mechanism, allows rapid adjustment of pattern period with subwavelength resolution, and retains the passive vibration-correction capability of Lloyd's mirror interferometers. Using this approach, we have successfully fabricated a grating structure with 112 nm period using a laser with 325 nm wavelength, attaining a numerical aperture of 1.45. The proposed immersion strategy can be adapted to improve pattern resolution of more complex interference lithography systems. © 2013 Optical Society of America

OCIS codes: (110.4235) Nanolithography; (220.4241) Nanostructure fabrication; (310.6628) Subwavelength structures, nanostructures.

<http://dx.doi.org/10.1364/OL.38.002531>

Periodic nanostructures are critical in many applications, including spectroscopy [1–3], subwavelength antireflection structures [4–6], superhydrophobic surfaces [6–8], and photonic/phononic crystals [9–12]. One attractive technique used to fabricate periodic nanostructures is laser interference lithography (IL) [12–17], where two or more mutually coherent laser beams interfere to create a periodic intensity pattern with high spatial-phase coherence over large areas. Recent work has shown the ability to pattern 300 mm substrates with subnanometer precision [15], as well as complex three-dimensional patterns [16]. The Lloyd's mirror IL (LIL) [18,19] method is another attractive IL implementation method with low hardware requirements. In this approach a mirror is used to create a virtual light source, allowing passive disturbance rejection and rapid period changes with little optics realignment [13,17]. However, these lithographic techniques are limited by the diffraction of light, and the smallest period that can be fabricated in air is roughly half of the wavelength $\lambda/2$.

There have been significant research efforts focusing on fabricating denser periodic nanostructures, as this can improve spectrometer resolution [1–3], surface properties [6], and surface-area-to-volume ratio. Shorter-wavelength light [20–22] can increase pattern resolution, but such light sources are not widely available and require costly diffractive/reflective optics. Multilevel IL has been demonstrated to pattern subwavelength structures [23], but this method requires multiple exposures and precise alignment. Another promising, straightforward approach to improve resolution is immersion lithography, which takes advantage of materials with high refractive index [24–28]. Recent works have successfully combined IL with solid immersion techniques to increase pattern resolution [26–28]. However, these methods require precisely machined prisms that can result in high setup cost. In addition, a thin layer of immersion fluid is required in these techniques to ensure

conformal contact between the prism and photoresist (PR), thereby limiting the spatial resolution to the fluid index.

In this work, we present an alternative all-liquid immersion approach based on a Lloyd's mirror interferometer. This method combines the higher refractive index of immersion fluid with the versatile configuration of a Lloyd's mirror interferometer to fabricate subwavelength periodic structures. The all-liquid approach ensures good conformal contact between the immersion fluid, the mirror, and the sample without any external mechanism. In addition, the system can be readily adjusted to fabricate a range of periods without extensive optical realignment. The proposed setup also maintains the passive vibration-isolation capability of a Lloyd's mirror interferometer to allow high exposure contrast.

The traditional LIL and the proposed liquid immersion system are illustrated in Fig. 1. The immersion Lloyd's mirror interference lithography (ILIL) setup consists of

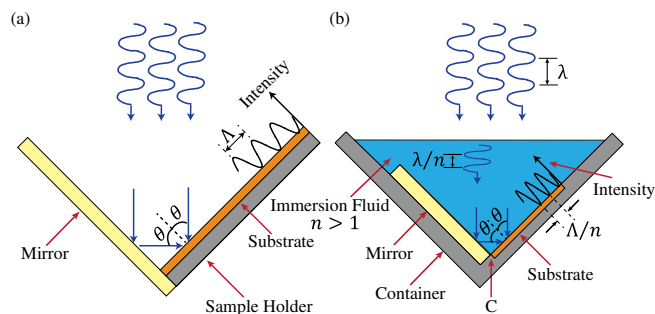


Fig. 1. (a) Schematic of standard LIL. Two beams interfere on the substrate to form a sinusoidal intensity pattern with period $\lambda/2 \sin \theta$. (b) Schematic of proposed ILIL setup with Lloyd's mirror interferometer in a fluid medium with high refractive index ($n > 1$). The period of sinusoidal intensity pattern formed on the substrate in the immersion fluid is reduced by a factor equal to the fluid index.

a mirror at 90° to the substrate holder, all mounted within a container filled with immersion fluid, as shown in Fig. 1(b). Resembling the Lloyd's mirror interferometer, the mirror and the substrate are always normal to each other and are allowed to rotate about point C to control incident angle. The wavelength of the normal-incidence UV light is reduced proportional to the refractive index of the fluid λ/n . The mirror forms a virtual light source, and the two light beams interfere on the substrate to form a one-dimensional (1D) sinusoidal intensity pattern. The PR records this intensity pattern with the period

$$\Lambda = \frac{\lambda}{2n \sin \theta}, \quad (1)$$

where λ is the exposure wavelength in air, θ is the incident angle, and n is the index of the immersion fluid. The container can be rotated around its axis to change the incidence angle, allowing facile period change without extensive system realignments. Note the laser is always at normal incidence to the air-liquid interface regardless of interference period. Gravity holds the immersion fluid against the mirror and substrate to produce conformal contact, reducing the formation of air pockets that can result in local defects. A flat glass plate is immersed in the liquid (not shown in the figure) to eliminate fluid ripples at the air-liquid interface. Careful loading and unloading of the sample is necessary to avoid formation of air bubbles in the immersion fluid. The all-liquid approach eliminates the need for precisely machined prisms and ensures conformal contact. Furthermore, the period can be configured by rotation of the entire setup, and the minimum period is a function of the immersion fluid index alone.

The samples for the ILIL exposure experiment are fabricated on silicon substrates. The substrates are coated with antireflection coating (ARC, Brewer Science i-CON-16, $n = 1.646 - 0.398j$) and a thin (50 nm) PR (PFI-88A2, $n = 1.72 - 0.04j$) to record the intensity pattern. The optimum ARC thickness for lowest power reflectivity at the resist interface is calculated using a multilayer thin-film model. ARC thickness between 80 and 120 nm is calculated to have minimal reflectivity for the incident angle range from 45° to 75° for both immersion fluids. The samples were exposed with a dose of 20 mJ and developed in 2.4% tetramethylammonium hydroxide developer solution (Microposit MF-CD-26) for 1–2 min.

The fabrication results using ILIL at different incident angles using deionized (DI) water ($n = 1.33$) and immersion oil ($n = 1.51$) are depicted in the top-view scanning electron microscope images shown in Fig. 2. A TE-polarized UV laser with wavelength of 325 nm is used for the exposure. The first sample has period of 170 nm and was patterned using DI water as immersion fluid for an incidence angle of 46° , as shown in Fig. 2(a). The structure period can be readily reduced by increasing the incidence angle, and smaller periods of 160 and 150 nm were patterned at incident angles of 50° and 54.5° , respectively. The use of higher-index immersion oil further reduces the grating period. Structure periods of 140, 130, and 120 nm were patterned at incident angles of 50.5° , 56° , and 64.5° , respectively, as shown in Figs. 2(d)–2(f).

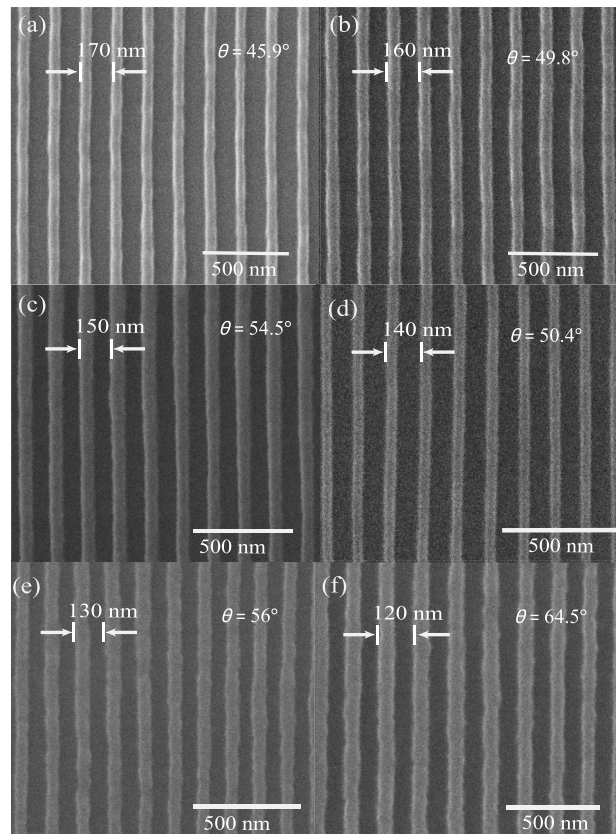


Fig. 2. Top view micrographs for fabrication results obtained using proposed ILIL setup at $\lambda = 325$ nm for (a)–(c) DI water ($n = 1.33$) and (d)–(f) immersion oil ($n = 1.51$) at various incident angles. Grating structures patterned in DI water with (a) 170 nm period at $\theta = 46^\circ$, (b) 160 nm period at $\theta = 49.8^\circ$, and (c) 150 nm period at $\theta = 54.5^\circ$. Grating structures patterned in immersion oil with (d) 140 nm period at $\theta = 50.5^\circ$, (e) 130 nm period at $\theta = 56^\circ$, and (f) 120 nm period at $\theta = 64.5^\circ$.

The sample is patterned uniformly with an area up to $50 \text{ mm} \times 50 \text{ mm}$, and the maximum area is limited by the size of the container used in the ILIL setup. A few point defects can be observed on the sample due to stationary dust particles within the fluid. Such particle contamination can be reduced by filtering the immersion fluids and conducting the experiments in a cleaner environment.

The smallest structure fabricated using the proposed ILIL method has a 112 nm period and was patterned at an incidence angle of 75° in immersion oil, as shown in Fig. 3. The structure was patterned using 325 nm wavelength light, thereby achieving a numerical aperture of 1.45. The cross-section micrograph of this sample is shown in Fig. 3(c), and high profile fidelity can be observed. At incident angles higher than 75° the oblique angle reduces the pattern area and fringe contrast, while the improvement of resolution is incremental. To obtain higher numerical aperture, immersion liquids with higher index can be used.

The smallest period that can be obtained is $\lambda/(2 * 1.51)$ using immersion fluid compared to $\lambda/2$ for nonimmersion IL. Using these data, the structure period can be plotted as a function of incident angle for the ILIL using air, water, and immersion oil, as illustrated in Fig. 4. The solid lines are a theoretical model of different immersion

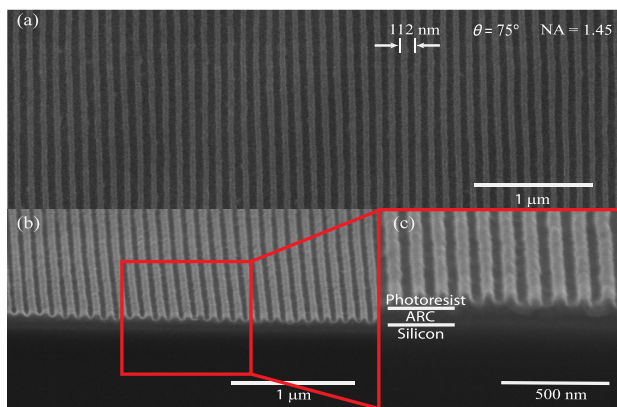


Fig. 3. Smallest grating period obtained using proposed setup with immersion oil with $n = 1.51$ and incidence angle of 75° , achieving a numerical aperture of 1.45. (a) Top view of the sample shows grating structure. (b) Cross-sectional view of the sample showing the profile of grating structure. (c) The materials used are indicated, with the formation of 1D periodic structure in the PR layer.

media derived using two-beam interference, as shown in Eq. (1). The experimental data agrees well with the model for both immersion fluids. The slight deviation of the data points from the numerical plot can be attributed to experimental uncertainty from manual adjustment error of incidence angle.

One important limitation for the ILIL approach is the optical absorption of the immersion fluid. While water is transparent at the exposure wavelength, higher-index immersion oil typically absorbs UV light. Since the optical path lengths are unequal in the ILIL configuration, absorption from immersion fluid can create amplitude imbalance for the two interference beams. This effect can result in fringe contrast reduction and linewidth variation, which will be more pronounced for sample areas away from the mirror. The absorption coefficient for the immersion oil used is experimentally measured to be 0.061 cm^{-1} , indicating a 10% reduction in contrast

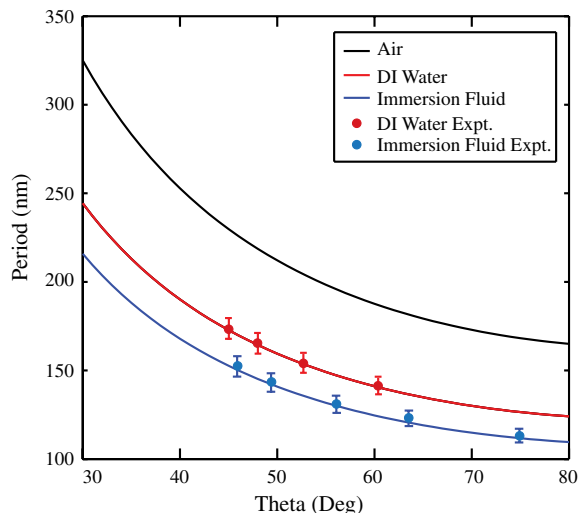


Fig. 4. Period reduction with the use of immersion fluid. Continuous lines show numerical model of grating period (Λ) as a function of angle of incidence (θ) for $\lambda = 325 \text{ nm}$. The discrete points are experimental results for respective immersion media.

across a 100 mm sample. Such contrast degradation is too small to be detected in the fabricated samples but can be a limiting factor for samples over 100 mm. With the proposed mechanism, it is possible to fabricate a grating structure with even smaller period by using immersion fluid with higher refractive index. We will explore the use of a 193 nm laser in this ILIL setup, given the commercially available immersion fluids at this wavelength.

In this work, an all-liquid IL technique based on the Lloyd's mirror is presented. This approach takes advantage of the high refractive index of immersion fluid to fabricate subwavelength periodic structures. We have successfully fabricated structures from 170 to 112 nm period using 325 nm wavelength, achieving a maximum numerical aperture of 1.45. The all-liquid approach ensures conformal contact between the immersion fluid, the mirror, and the substrate, which helps to reduce possible defects in the final grating structure. Rapid tunability of the setup to the desired angle provides the ability to fabricate a range of subwavelength periodic structures with high fidelity. This method can be extended to fabricate 2D structures and is being explored.

We gratefully acknowledge the students, staff, and facility support from the North Carolina State University Nanofabrication Facility (NNF). This work was supported by a NASA Office of the Chief Technologist's Space Technology Research Opportunity—Early Career Faculty grant (grant NNX12AQ46G).

References

- R. K. Heilmann, M. Ahn, A. Brucocoleri, C.-H. Chang, E. M. Gullikson, P. Mukherjee, and M. L. Schattenburg, *Appl. Opt.* **50**, 1364 (2011).
- C. Braig, T. Käsebier, E.-B. Kley, and A. Tünnermann, *Opt. Express* **19**, 14008 (2011).
- R. K. Heilmann, M. Ahn, E. M. Gullikson, and M. L. Schattenburg, *Opt. Express* **16**, 8658 (2008).
- A. R. Parker and H. E. Townley, *Nat. Nanotechnol.* **2**, 347 (2007).
- Y.-F. Huang, S. Chattopadhyay, Y.-J. Jen, C.-Y. Peng, T.-A. Liu, Y.-K. Hsu, C.-L. Pan, H.-C. Lo, C.-H. Hsu, Y.-H. Chang, C.-S. Lee, K.-H. Chen, and L.-C. Chen, *Nat. Nanotechnol.* **2**, 770 (2007).
- K.-C. Park, H. J. Choi, C.-H. Chang, R. E. Cohen, G. H. McKinley, and G. Barbastathis, *ACS Nano* **6**, 3789 (2012).
- K. Liu and L. Jiang, *Nano Today* **6**(2), 155 (2011).
- D. Wu, Q.-D. Chen, H. Xia, J. Jiao, B.-B. Xu, X.-F. Lin, Y. Xu, and H.-B. Sun, *Soft Mater.* **6**, 263 (2010).
- S. Y. Lin, J. G. Fleming, D. L. Hetherington, B. K. Smith, R. Biswas, K. M. Ho, M. M. Sigalas, W. Zubrzycki, S. R. Kurtz, and J. Bur, *Nature* **394**, 251 (1998).
- S. Noda, K. Tomoda, N. Yamamoto, and A. Chutinan, *Science* **289**, 604 (2000).
- M. Qi, E. Lidorikis, P. T. Rakich, S. G. Johnson, J. D. Joannopoulos, E. P. Ippen, and H. I. Smith, *Nature* **429**, 538 (2004).
- J.-H. Jang, C. K. Ullal, T. Gorishnyy, V. V. Tsukruk, and E. L. Thomas, *Nano Lett.* **6**, 740 (2006).
- H. I. Smith, *Phys. E* **11**, 104 (2001).
- C. G. Chen, P. T. Konkola, R. K. Heilmann, C. Joo, and M. L. Schattenburg, *Proc. SPIE* **4936**, 126 (2002).
- R. K. Heilmann, C. G. Chen, P. T. Konkola, and M. L. Schattenburg, *Nanotechnology* **15**, S504 (2004).

16. J.-H. Jang, C. K. Ullal, M. Maldovan, T. Gorishnyy, S. Kooi, C. Koh, and E. L. Thomas, *Adv. Funct. Mater.* **17**, 3027 (2007).
17. T. B. O'Reilly and H. I. Smith, *J. Vac. Sci. Technol. B* **26**, 2131 (2008).
18. J. de Boor, N. Geyer, U. Gösele, and V. Schmidt, *Opt. Lett.* **34**, 1783 (2009).
19. I. Wathuthanthri, W. Mao, and C.-H. Choi, *Opt. Lett.* **36**, 1593 (2011).
20. H. H. Solak, *J. Phys. D* **39**, R171 (2006).
21. A. Ritucci, A. Reale, P. Zuppella, L. Reale, P. Tucceri, G. Tomassetti, P. Bettotti, and L. Pavesi, *J. Appl. Phys.* **102**, 034313 (2007).
22. P. W. Wachulak, M. G. Capeluto, M. C. Marconi, C. S. Menoni, and J. J. Rocca, *Opt. Express* **15**, 3465 (2007).
23. C.-H. Chang, Y. Zhao, R. K. Heilmann, and M. L. Schattenburg, *Opt. Lett.* **33**, 1572 (2008).
24. R. French, *Annu. Rev. Mater. Res.* **39**, 93 (2009).
25. Y. Wei and R. L. Brainard, *Advanced Processes for 193 nm Immersion Lithography* (SPIE, 2009).
26. J. de Boor, D. S. Kim, and V. Schmidt, *Opt. Lett.* **35**, 3450 (2010).
27. T. M. Bloomstein, M. F. Marchant, S. Deneault, D. E. Hardy, and M. Rothschild, *Opt. Express* **14**, 6434 (2006).
28. P. Mehrotra, C. W. Holzwarth, and R. J. Blaikie, *J. Microlithogr. Microfabr. Microsyst.* **10**, 033012 (2011).